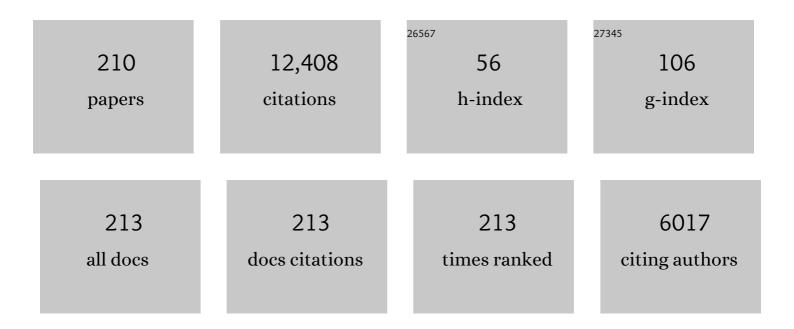
## **Ulf Helmersson**

List of Publications by Year in descending order

Source: https://exaly.com/author-pdf/3230859/publications.pdf Version: 2024-02-01



#	Article	IF	CITATIONS
1	A novel pulsed magnetron sputter technique utilizing very high target power densities. Surface and Coatings Technology, 1999, 122, 290-293.	2.2	910
2	Ionized physical vapor deposition (IPVD): A review of technology and applications. Thin Solid Films, 2006, 513, 1-24.	0.8	886
3	Growth of singleâ€crystal TiN/VN strainedâ€layer superlattices with extremely high mechanical hardness. Journal of Applied Physics, 1987, 62, 481-484.	1.1	714
4	High power impulse magnetron sputtering discharge. Journal of Vacuum Science and Technology A: Vacuum, Surfaces and Films, 2012, 30, .	0.9	568
5	On the film density using high power impulse magnetron sputtering. Surface and Coatings Technology, 2010, 205, 591-596.	2.2	317
6	Microstructure modification of TiN by ion bombardment during reactive sputter deposition. Thin Solid Films, 1989, 169, 299-314.	0.8	308
7	Optical properties of anatase TiO2 thin films prepared by aqueous sol–gel process at low temperature. Thin Solid Films, 2002, 405, 50-54.	0.8	286
8	The ion energy distributions and ion flux composition from a high power impulse magnetron sputtering discharge. Thin Solid Films, 2006, 515, 1522-1526.	0.8	279
9	Influence of high power densities on the composition of pulsed magnetron plasmas. Vacuum, 2002, 65, 147-154.	1.6	268
10	High power pulsed magnetron sputtered CrN films. Surface and Coatings Technology, 2003, 163-164, 267-272.	2.2	242
11	Ionized sputter deposition using an extremely high plasma density pulsed magnetron discharge. Journal of Vacuum Science and Technology A: Vacuum, Surfaces and Films, 2000, 18, 1533-1537.	0.9	235
12	lonization of sputtered metals in high power pulsed magnetron sputtering. Journal of Vacuum Science and Technology A: Vacuum, Surfaces and Films, 2005, 23, 18-22.	0.9	214
13	Ion-assisted physical vapor deposition for enhanced film properties on nonflat surfaces. Journal of Vacuum Science and Technology A: Vacuum, Surfaces and Films, 2005, 23, 278-280.	0.9	211
14	Comparison of microstructure and mechanical properties of chromium nitride-based coatings deposited by high power impulse magnetron sputtering and by the combined steered cathodic arc/unbalanced magnetron technique. Thin Solid Films, 2004, 457, 270-277.	0.8	196
15	Spatial and temporal behavior of the plasma parameters in a pulsed magnetron discharge. Surface and Coatings Technology, 2002, 161, 249-256.	2.2	189
16	A spectroscopic ellipsometry study of cerium dioxide thin films grown on sapphire by rf magnetron sputtering. Journal of Applied Physics, 1995, 77, 5369-5376.	1.1	186
17	Lowâ€Temperature Superionic Conductivity in Strained Yttriaâ€Stabilized Zirconia. Advanced Functional Materials, 2010, 20, 2071-2076.	7.8	150
18	Evolution of the electron energy distribution and plasma parameters in a pulsed magnetron discharge. Applied Physics Letters, 2001, 78, 3427-3429.	1.5	141

#	Article	IF	CITATIONS
19	Adhesion of titanium nitride coatings on highâ€speed steels. Journal of Vacuum Science and Technology A: Vacuum, Surfaces and Films, 1985, 3, 308-315.	0.9	131
20	Investigation of high power impulse magnetron sputtering pretreated interfaces for adhesion enhancement of hard coatings on steel. Surface and Coatings Technology, 2006, 200, 6495-6499.	2.2	131
21	Hysteresis-free reactive high power impulse magnetron sputtering. Thin Solid Films, 2008, 516, 6398-6401.	0.8	123
22	Lowâ€energy ion irradiation during film growth for reducing defect densities in epitaxial TiN(100) films deposited by reactiveâ€magnetron sputtering. Journal of Applied Physics, 1987, 61, 552-555.	1.1	110
23	Cross-field ion transport during high power impulse magnetron sputtering. Plasma Sources Science and Technology, 2008, 17, 035021.	1.3	106
24	Phase tailoring of Ta thin films by highly ionized pulsed magnetron sputtering. Thin Solid Films, 2007, 515, 3434-3438.	0.8	104
25	Low temperature deposition of α-Al[sub 2]O[sub 3] thin films by sputtering using a Cr[sub 2]O[sub 3] template. Journal of Vacuum Science and Technology A: Vacuum, Surfaces and Films, 2002, 20, 2134.	0.9	103
26	Fully dense, non-faceted 111-textured high power impulse magnetron sputtering TiN films grown in the absence of substrate heating and bias. Thin Solid Films, 2010, 518, 5978-5980.	0.8	101
27	Spatial electron density distribution in a high-power pulsed magnetron discharge. IEEE Transactions on Plasma Science, 2005, 33, 346-347.	0.6	100
28	Microstructure of α-alumina thin films deposited at low temperatures on chromia template layers. Journal of Vacuum Science and Technology A: Vacuum, Surfaces and Films, 2004, 22, 117-121.	0.9	99
29	Plasma dynamics in a highly ionized pulsed magnetron discharge. Plasma Sources Science and Technology, 2005, 14, 525-531.	1.3	98
30	A strategy for increased carbon ionization in magnetron sputtering discharges. Diamond and Related Materials, 2012, 23, 1-4.	1.8	97
31	High-power impulse magnetron sputtering of Ti–Si–C thin films from a Ti3SiC2 compound target. Thin Solid Films, 2006, 515, 1731-1736.	0.8	96
32	Phase control of Al2O3 thin films grown at low temperatures. Thin Solid Films, 2006, 513, 57-59.	0.8	91
33	Growth and field dependent dielectric properties of epitaxial Na0.5K0.5NbO3 thin films. Applied Physics Letters, 1998, 73, 927-929.	1.5	90
34	Guiding the deposition flux in an ionized magnetron discharge. Thin Solid Films, 2006, 515, 1928-1931.	0.8	88
35	Understanding the discharge current behavior in reactive high power impulse magnetron sputtering of oxides. Journal of Applied Physics, 2013, 113, .	1.1	86
36	Effects of substrate temperature and substrate material on the structure of reactively sputtered TiN films. Thin Solid Films, 1984, 122, 115-129.	0.8	83

#	Article	IF	CITATIONS
37	Synthesis of α-Al <sub>2</sub> O <sub>3</sub> thin films using reactive high-power impulse magnetron sputtering. Europhysics Letters, 2008, 82, 36002.	0.7	82
38	Hysteresis and process stability in reactive high power impulse magnetron sputtering of metal oxides. Thin Solid Films, 2011, 519, 7779-7784.	0.8	82
39	Transition between the discharge regimes of high power impulse magnetron sputtering and conventional direct current magnetron sputtering. Plasma Sources Science and Technology, 2009, 18, 045008.	1.3	79
40	Cross-Section preparation for tem of film-substrate combinations with a large difference in sputtering yields. Journal of Electron Microscopy Technique, 1986, 4, 361-369.	1.1	76
41	Microstructure evolution in TiN films reactively sputter deposited on multiphase substrates. Journal of Vacuum Science and Technology A: Vacuum, Surfaces and Films, 1986, 4, 500-503.	0.9	76
42	On the electron energy in the high power impulse magnetron sputtering discharge. Journal of Applied Physics, 2009, 105, .	1.1	76
43	Room temperature deposition of homogeneous, highly transparent and conductive Al-doped ZnO films by reactive high power impulse magnetron sputtering. Solar Energy Materials and Solar Cells, 2016, 157, 742-749.	3.0	74
44	Hydrogen uptake in alumina thin films synthesized from an aluminum plasma stream in an oxygen ambient. Applied Physics Letters, 1999, 74, 200-202.	1.5	73
45	Effect of peak power in reactive high power impulse magnetron sputtering of titanium dioxide. Surface and Coatings Technology, 2011, 205, 4828-4831.	2.2	70
46	Bipolar HiPIMS for tailoring ion energies in thin film deposition. Surface and Coatings Technology, 2019, 359, 433-437.	2.2	70
47	Sharp microfaceting of (001)-oriented cerium dioxide thin films and the effect of annealing on surface morphology. Surface Science, 1999, 429, 22-33.	0.8	68
48	Measurement of the magnetic field change in a pulsed high current magnetron discharge. Plasma Sources Science and Technology, 2004, 13, 654-661.	1.3	64
49	Understanding deposition rate loss in high power impulse magnetron sputtering: I. Ionization-driven electric fields. Plasma Sources Science and Technology, 2012, 21, 025005.	1.3	64
50	Reactively magnetron sputtered Hfâ€N films. II. Hardness and electrical resistivity. Journal of Applied Physics, 1985, 58, 3112-3117.	1.1	61
51	Yttrium oxide inclusions in YBa2Cu3Ox thin films. Physica C: Superconductivity and Its Applications, 1992, 202, 69-74.	0.6	61
52	Energy flux measurements in high power impulse magnetron sputtering. Journal Physics D: Applied Physics, 2009, 42, 185202.	1.3	60
53	Studies of hysteresis effect in reactive HiPIMS deposition of oxides. Surface and Coatings Technology, 2011, 205, S303-S306.	2.2	59
54	Anomalous electron transport in high power impulse magnetron sputtering. Plasma Sources Science and Technology, 2008, 17, 025007.	1.3	58

#	Article	IF	CITATIONS
55	Growth of Ti-C nanocomposite films by reactive high power impulse magnetron sputtering under industrial conditions. Surface and Coatings Technology, 2012, 206, 2396-2402.	2.2	58
56	ZrB2 thin films grown by high power impulse magnetron sputtering from a compound target. Thin Solid Films, 2012, 526, 163-167.	0.8	58
57	Growth, structural characterization and properties of hard and wear-protective layered materials. Thin Solid Films, 1990, 193-194, 818-831.	0.8	55
58	Sol–gel synthesis and characterization of Na0.5K0.5NbO3 thin films. Journal of Crystal Growth, 2005, 281, 468-474.	0.7	54
59	Microstructural and microchemical characterization of hard coatings. Journal of Vacuum Science and Technology A: Vacuum, Surfaces and Films, 1986, 4, 2770-2783.	0.9	53
60	Structure and ammonia sensitivity of thin platinum or iridium gates in metal-oxide-silicon capacitors. Thin Solid Films, 1989, 177, 77-93.	0.8	53
61	Electrical properties of SrTiO3 thin films on Si deposited by magnetron sputtering at low temperature. Applied Physics Letters, 2001, 79, 1513-1515.	1.5	53
62	Energy distributions of positive and negative ions during magnetron sputtering of an Al target in Arâ^•O2 mixtures. Journal of Applied Physics, 2006, 100, 033305.	1.1	53
63	Highly reflective rear surface passivation design for ultra-thin Cu(In,Ga)Se 2 solar cells. Thin Solid Films, 2015, 582, 300-303.	0.8	51
64	Formation of Cuâ€rich particles on the surface of YBa2Cu3O7â^'xthin film grown byinsituoffâ€axis sputtering. Journal of Applied Physics, 1994, 75, 2020-2025.	1.1	50
65	A nanostructured NiO/cubic SiC p–n heterojunction photoanode for enhanced solar water splitting. Journal of Materials Chemistry A, 2019, 7, 4721-4728.	5.2	50
66	Faster-than-Bohm Cross- <mml:math <br="" xmlns:mml="http://www.w3.org/1998/Math/MathML">display="inline"&gt;<mml:mi>B</mml:mi></mml:math> Electron Transport in Strongly Pulsed Plasmas. Physical Review Letters, 2009, 103, 225003.	2.9	49
67	A bulk plasma model for dc and HiPIMS magnetrons. Plasma Sources Science and Technology, 2008, 17, 045009.	1.3	48
68	Reactively magnetron sputtered Hfâ€N films. I. Composition and structure. Journal of Applied Physics, 1985, 58, 3104-3111.	1.1	46
69	Resputtering effects on the stoichiometry of YBa2Cu3Oxthin films. Journal of Applied Physics, 1991, 69, 390-395.	1.1	46
70	HTS/ferroelectric devices for microwave applications. IEEE Transactions on Applied Superconductivity, 1997, 7, 2458-2461.	1.1	46
71	Modelling of thin-film HTS/ferroelectric interdigital capacitors. IET Microwaves Antennas and Propagation, 1996, 143, 397.	1.2	44
72	Compressive intrinsic stress originates in the grain boundaries of dense refractory polycrystalline thin films. Journal of Applied Physics, 2016, 119, .	1.1	44

#	Article	IF	CITATIONS
73	Structure of reactively magnetron sputtered Hfâ€N films. Applied Physics Letters, 1984, 44, 670-672.	1.5	43
74	Eliminating the hysteresis effect for reactive sputtering processes. Applied Physics Letters, 2005, 86, 164106.	1.5	43
75	High rate reactive dc magnetron sputter deposition of Al2O3 films. Journal of Vacuum Science and Technology A: Vacuum, Surfaces and Films, 1998, 16, 639-643.	0.9	42
76	Ab initiostudies of Al, O, and O2adsorption on Î $\pm$ â''Al2O3(0001) surfaces. Physical Review B, 2006, 74, .	1.1	42
77	Size-controlled growth of nanoparticles in a highly ionized pulsed plasma. Applied Physics Letters, 2013, 102, .	1.5	42
78	Initial growth of TiN on different phases of high speed steel. Thin Solid Films, 1985, 124, 163-170.	0.8	41
79	Composition, structure, and dielectric tunability of epitaxial SrTiO3 thin films grown by radio frequency magnetron sputtering. Journal of Vacuum Science and Technology A: Vacuum, Surfaces and Films, 1999, 17, 564-570.	0.9	41
80	Carbon Monoxide Oxidation on Copper Oxide Thin Films Supported on Corrugated Cerium Dioxide {111} and {001} Surfaces. Journal of Catalysis, 1999, 181, 6-15.	3.1	41
81	The role of Ohmic heating in dc magnetron sputtering. Plasma Sources Science and Technology, 2016, 25, 065024.	1.3	41
82	α-Alumina coatings on WC/Co substrates by physical vapor deposition. International Journal of Refractory Metals and Hard Materials, 2009, 27, 507-512.	1.7	37
83	Plasma characteristics at off-axis high pressure magnetron YBa2Cu3O7â~î^ sputtering. Journal of Applied Physics, 1997, 82, 1882-1889.	1.1	36
84	lon-acoustic solitary waves in a high power pulsed magnetron sputtering discharge. Journal Physics D: Applied Physics, 2005, 38, 3417-3421.	1.3	36
85	Internal current measurements in high power impulse magnetron sputtering. Plasma Sources Science and Technology, 2011, 20, 045003.	1.3	35
86	Structural characterization of yttria (Y2O3) inclusions in YBa2Cu3O7â^'x films: Growth model and effect on critical current density. Thin Solid Films, 1993, 229, 237-248.	0.8	34
87	Epitaxial growth of W-doped VO2/V2O3 multilayer on α-Al2O3(110) by reactive magnetron sputtering. Thin Solid Films, 2000, 375, 128-131.	0.8	34
88	Evaluation of Intermittent Contact Mode AFM Probes by HREM and Using Atomically Sharp CeO2Ridges as Tip Characterizer. Langmuir, 2000, 16, 6267-6277.	1.6	34
89	Fast growth of nanoparticles in a hollow cathode plasma through orbit motion limited ion collection. Applied Physics Letters, 2013, 103, 193108.	1.5	33
90	Effects of additives in α- and Î,-alumina: an ab initio study. Journal of Physics Condensed Matter, 2004, 16, 8971-8980.	0.7	32

#	Article	IF	CITATIONS
91	Target presputtering effects on stoichiometry and deposition rate of Yâ€Baâ€Cuâ€O thin films grown by dc magnetron sputtering. Applied Physics Letters, 1988, 52, 1907-1909.	1.5	30
92	Elastic modulus-density relationship for amorphous boron suboxide thin films. Applied Physics A: Materials Science and Processing, 2003, 76, 269-271.	1.1	30
93	Bipolar high power impulse magnetron sputtering for energetic ion bombardment during TiN thin film growth without the use of a substrate bias. Thin Solid Films, 2019, 688, 137350.	0.8	30
94	Magnetoconductivity inYBa2Cu3O7â^îîthin films. Physical Review B, 1995, 52, 3748-3755.	1.1	28
95	Microstructure and microwave dielectric properties of epitaxial SrTiO3 films on LaAlO3 substrates. Journal of Applied Physics, 1998, 83, 4884-4890.	1.1	28
96	Epitaxial cerium oxide buffer layers and YBa <sub>2</sub> Cu <sub>3</sub> O <sub>7â^îî</sub> thin films for microwave device applications. Journal of Materials Research, 1999, 14, 2385-2393.	1.2	28
97	Influence of residual water on magnetron sputter deposited crystalline Al2O3 thin films. Thin Solid Films, 2008, 516, 3877-3883.	0.8	28
98	Influence of ionization degree on film properties when using high power impulse magnetron sputtering. Journal of Vacuum Science and Technology A: Vacuum, Surfaces and Films, 2012, 30, .	0.9	28
99	Determination of the complex dielectric function of epitaxial SrTiO3 films using transmission electron energy-loss spectroscopy. Journal of Applied Physics, 1999, 85, 2828-2834.	1.1	27
100	Radio frequency dual magnetron sputtering deposition and characterization of nanocomposite Al2O3–ZrO2 thin films. Journal of Vacuum Science and Technology A: Vacuum, Surfaces and Films, 2006, 24, 309-316.	0.9	27
101	Dual-magnetron open field sputtering system for sideways deposition of thin films. Surface and Coatings Technology, 2010, 204, 2165-2169.	2.2	27
102	Growth and characterization of epitaxial films of tungsten-doped vanadium oxides on sapphire (110) by reactive magnetron sputtering. Journal of Vacuum Science and Technology A: Vacuum, Surfaces and Films, 1999, 17, 1817-1821.	0.9	25
103	Ab initiocalculations on the effects of additives on alumina phase stability. Physical Review B, 2005, 71,	1.1	25
104	Performance tuning of gas sensors based on epitaxial graphene on silicon carbide. Materials and Design, 2018, 153, 153-158.	3.3	25
105	Effect of substrate temperature on the deposition of Al-doped ZnO thin films using high power impulse magnetron sputtering. Surface and Coatings Technology, 2018, 347, 245-251.	2.2	25
106	High resolution X-ray diffraction mapping studies on the domain structure of LaAlO3 single crystal substrates and its influence on SrTiO3 film growth. Journal of Crystal Growth, 1997, 171, 401-408.	0.7	24
107	Peroxo sol–gel preparation: photochromic/electrochromic properties of Mo–Ti oxide gels and thin films. Journal of Materials Chemistry, 2000, 10, 2396-2400.	6.7	24
108	High Li+-Ion Storage Capacity and Double-Electrochromic Behavior of Solâ^'Gel-Derived Iron Oxide Thin Films with Sulfate Residues. Chemistry of Materials, 2001, 13, 1976-1983.	3.2	24

#	Article	IF	CITATIONS
109	Synthesis and mechanical properties of boron suboxide thin films. Journal of Vacuum Science and Technology A: Vacuum, Surfaces and Films, 2002, 20, 335-337.	0.9	24
110	Growth and Characterization of Na <sub>0.5</sub> K <sub>0.5</sub> NbO <sub>3</sub> Thin Films on Polycrystalline Pt <sub>80</sub> Ir <sub>20</sub> Substrates. Journal of Materials Research, 2002, 17, 1183-1191.	1.2	24
111	Deposition of yttria-stabilized zirconia thin films by high power impulse magnetron sputtering and pulsed magnetron sputtering. Surface and Coatings Technology, 2014, 240, 1-6.	2.2	24
112	Low-energy ion irradiation in HiPIMS to enable anatase TiO <sub>2</sub> selective growth. Journal Physics D: Applied Physics, 2018, 51, 235301.	1.3	24
113	Low-Loss and Tunable Localized Mid-Infrared Plasmons in Nanocrystals of Highly Degenerate InN. Nano Letters, 2018, 18, 5681-5687.	4.5	24
114	Pulse length selection for optimizing the accelerated ion flux fraction of a bipolar HiPIMS discharge. Plasma Sources Science and Technology, 2020, 29, 125013.	1.3	24
115	Low temperature ( <i>T</i> s/ <i>T</i> m &lt; 0.1) epitaxial growth of HfN/MgO(001) via reactive HiPII with metal-ion synchronized substrate bias. Journal of Vacuum Science and Technology A: Vacuum, Surfaces and Films, 2018, 36, .	MS 0.9	23
116	Process stabilization by peak current regulation in reactive high-power impulse magnetron sputtering of hafnium nitride. Journal Physics D: Applied Physics, 2016, 49, 065202.	1.3	22
117	Graphene Decorated with Iron Oxide Nanoparticles for Highly Sensitive Interaction with Volatile Organic Compounds. Sensors, 2019, 19, 918.	2.1	22
118	Synthesis of titanium-oxide nanoparticles with size and stoichiometry control. Journal of Nanoparticle Research, 2015, 17, 1.	0.8	21
119	Electronic properties of epitaxial TiN/VN(001) superlattices. Journal of Applied Physics, 1991, 70, 4963-4968.	1.1	20
120	Morphology changes of thin Pd films grown on SiO 2 : influence of adsorbates and temperature. Thin Solid Films, 1999, 342, 297-306.	0.8	19
121	Time-domain and energetic bombardment effects on the nucleation and coalescence of thin metal films on amorphous substrates. Journal Physics D: Applied Physics, 2013, 46, 215303.	1.3	19
122	Reduction of surface particles on YBa2Cu3O7â^â,thin films through the use of nonstoichiometric sputtering targets and N2O in the sputtering gas. Journal of Applied Physics, 1995, 77, 6388-6393.	1.1	18
123	Monte Carlo simulations of the transport of sputtered particles. Computer Physics Communications, 1999, 120, 238-254.	3.0	18
124	Low temperature growth and characterization of (Na,K)NbOx thin films. Journal of Crystal Growth, 2003, 254, 400-404.	0.7	18
125	Elastic modulus of amorphous boron suboxide thin films studied by theoretical and experimental methods. Journal of Applied Physics, 2003, 93, 940-944.	1.1	18
126	Two-domain formation during the epitaxial growth of GaN (0001) on <i>c</i> -plane Al2O3 (0001) by high power impulse magnetron sputtering. Journal of Applied Physics, 2011, 110, .	1.1	18

#	Article	IF	CITATIONS
127	Synthesis of hydrogenated diamondlike carbon thin films using neon–acetylene based high power impulse magnetron sputtering discharges. Journal of Vacuum Science and Technology A: Vacuum, Surfaces and Films, 2016, 34, 061504.	0.9	18
128	Experimental verification of deposition rate increase, with maintained high ionized flux fraction, by shortening the HiPIMS pulse. Plasma Sources Science and Technology, 2021, 30, 045006.	1.3	18
129	Flux pinning in YBa2Cu3O7 thin films grown by d.c. magnetron sputtering. Cryogenics, 1992, 32, 1084-1088.	0.9	17
130	X-ray-diffraction mapping of epitaxialYBa2Cu3O7â^'xthin films: Determination of in-plane epitaxy anda-,b-, andc-axis lengths in films with varying oxygen deficiency. Physical Review B, 1993, 47, 3431-3434.	1.1	17
131	Stabilization of potential superhardRuO2phases: A theoretical study. Physical Review B, 2002, 66, .	1.1	17
132	Modeling the extraction of sputtered metal from high power impulse hollow cathode discharges. Plasma Sources Science and Technology, 2013, 22, 035006.	1.3	17
133	Microstructure/dielectric property relationship of low temperature synthesised (Na,K)NbOx thin films. Journal of Crystal Growth, 2004, 262, 322-326.	0.7	16
134	Principles for designing sputtering-based strategies for high-rate synthesis of dense and hard hydrogenated amorphous carbon thin films. Diamond and Related Materials, 2014, 44, 117-122.	1.8	16
135	Catalytic Nanotruss Structures Realized by Magnetic Self-Assembly in Pulsed Plasma. Nano Letters, 2018, 18, 3132-3137.	4.5	16
136	Bipolar HiPIMS: The role of capacitive coupling in achieving ion bombardment during growth of dielectric thin films. Surface and Coatings Technology, 2021, 416, 127152.	2.2	16
137	Copper thin films deposited using different ion acceleration strategies in HiPIMS. Surface and Coatings Technology, 2021, 422, 127487.	2.2	16
138	Electrical characterisation of SrTiO3/Si interfaces. Journal of Non-Crystalline Solids, 2002, 303, 185-189.	1.5	14
139	The influence of pressure and gas flow on size and morphology of titanium oxide nanoparticles synthesized by hollow cathode sputtering. Journal of Applied Physics, 2016, 120, 044308.	1.1	14
140	Structural and electrical characterization of sputter-deposited SrTiO3 thin films. Microelectronic Engineering, 1995, 29, 123-127.	1.1	13
141	Reduction of density of subgrain boundaries and misfit dislocations in epitaxial (001) SrTiO3 thin films: Effect on dielectric tunability. Journal of Applied Physics, 1999, 85, 3976-3983.	1.1	12
142	Influence of high-energy Si+ ion irradiation on microstructure and mechanical properties of alumina films. Surface and Coatings Technology, 2002, 158-159, 534-537.	2.2	12
143	Deep energy levels in RuO2â^•4H–SiC Schottky barrier structures. Applied Physics Letters, 2006, 88, 153509.	1.5	12
144	Investigation of RuO2/4H–SiC Schottky diode contacts by deep level transient spectroscopy. Chemical Physics Letters, 2006, 429, 617-621.	1.2	11

#	Article	IF	CITATIONS
145	Low-temperature α-alumina thin film growth:ab initiostudies of Al adatom surface migration. Journal Physics D: Applied Physics, 2009, 42, 125302.	1.3	11
146	Formation of secondary phases in YBa2Cu3O7â^'Î/SrTiO3 multilayers. Physica C: Superconductivity and Its Applications, 1998, 304, 245-254.	0.6	10
147	Modeling of the deposition of stoichiometric Al2O3 using nonarcing direct current magnetron sputtering. Journal of Vacuum Science and Technology A: Vacuum, Surfaces and Films, 1998, 16, 1286-1292.	0.9	10
148	Growth of SrTiO3 thin films on LaAlO3(001) substrates; the influence of growth temperature on composition, orientation, and surface morphology. Thin Solid Films, 2000, 360, 181-186.	0.8	10
149	Role of carbon in boron suboxide thin films. Journal of Vacuum Science and Technology A: Vacuum, Surfaces and Films, 2003, 21, 1355-1358.	0.9	10
150	Molecular content of the deposition flux during reactive Arâ^•O2 magnetron sputtering of Al. Applied Physics Letters, 2006, 88, 054101.	1.5	10
151	Ab initio calculations and synthesis of the off-stoichiometric half-Heusler phase Ni1â^'xMn1+xSb. Journal of Applied Physics, 2010, 108, 093712.	1.1	10
152	Restoring the Properties of Transparent Al-Doped ZnO Thin Film Electrodes Exposed to Ambient Air. Journal of Physical Chemistry C, 2017, 121, 14426-14433.	1.5	10
153	Low temperature growth of stress-free single phase <i>α</i> -W films using HiPIMS with synchronized pulsed substrate bias. Journal of Applied Physics, 2021, 129, .	1.1	10
154	Dynamics of bipolar HiPIMS discharges by plasma potential probe measurements. Plasma Sources Science and Technology, 2022, 31, 025007.	1.3	10
155	Dislocations, strain, and defects in heteroepitaxial YBa2Cu3O7â^x/SrTiO3 multilayers. Physica C: Superconductivity and Its Applications, 1998, 304, 307-313.	0.6	9
156	Growth of semi-coherent Ni and NiO dual-phase nanoparticles using hollow cathode sputtering. Journal of Nanoparticle Research, 2019, 21, 1.	0.8	9
157	Pt/CeO2 SIC Schottky diodes with high response to hydrogen and hydrocarbons. , 2001, , 832-835.		9
158	Magnetically Collected Platinum/Nickel Alloy Nanoparticles as Catalysts for Hydrogen Evolution. ACS Applied Nano Materials, 2021, 4, 12957-12965.	2.4	9
159	The effect of oxygen and substrate temperature on the growth of Ti thin films on stainlessâ€steel substrates. Journal of Vacuum Science and Technology A: Vacuum, Surfaces and Films, 1983, 1, 301-304.	0.9	8
160	Modified Epitaxial Graphene on SiC for Extremely Sensitive and Selective Gas Sensors. Materials Science Forum, 2016, 858, 1145-1148.	0.3	8
161	The use of Highly Ionized Pulsed Plasmas for the Synthesis of Advanced Thin Films and Nanoparticles. KONA Powder and Particle Journal, 2014, 31, 171-180.	0.9	7
162	Roomâ€Temperature Micropillar Growth of Lithium–Titanate–Carbon Composite Structures by Selfâ€Biased Direct Current Magnetron Sputtering for Lithium Ion Microbatteries. Advanced Functional Materials, 2019, 29, 1904306.	7.8	7

#	Article	IF	CITATIONS
163	Tuning the stress in TiN films by regulating the doubly charged ion fraction in a reactive HiPIMS discharge. Journal of Applied Physics, 2020, 127, .	1.1	7
164	Observation of metallic resistivity behavior following a 1/i̇̀300Kdependence ofTcin aYBa2Cu3O7â^'xthin film with varyingab initioxygen deficiency. Physical Review B, 1993, 48, 7708-7711.	1.1	6
165	Characteristics of SrTiO <sub>3</sub> thin films deposited on Si by rf magnetron sputtering at various substrate temperatures. The Philosophical Magazine: Physics of Condensed Matter B, Statistical Mechanics, Electronic, Optical and Magnetic Properties, 2002, 82, 891-903.	0.6	6
166	Properties of Al–SrTiO <tex>\$_3\$</tex> –ITO Capacitors for Microelectronic Device Applications. IEEE Transactions on Electron Devices, 2004, 51, 1202-1205.	1.6	6
167	Double oxide shell layer formed on a metal nanoparticle as revealed by aberration corrected (scanning) transmission electron microscopy. Materials Research Express, 2014, 1, 025016.	0.8	6
168	Characteristics of SrTiO 3 thin films deposited on Si by rf magnetron sputtering at various substrate temperatures. The Philosophical Magazine: Physics of Condensed Matter B, Statistical Mechanics, Electronic, Optical and Magnetic Properties, 2002, 82, 891-903.	0.6	6
169	Molecular dynamics simulation of the growth of Cu nanoclusters from Cu ions in a plasma. Physical Review B, 2014, 90, .	1.1	5
170	Nanoparticle growth by collection of ions: orbital motion limited theory and collision-enhanced collection. Journal Physics D: Applied Physics, 2016, 49, 395208.	1.3	5
171	Impact of nanoparticle magnetization on the 3D formation of dual-phase Ni/NiO nanoparticle-based nanotrusses. Journal of Nanoparticle Research, 2019, 21, 1.	0.8	5
172	Summary Abstract: The role of lowâ€energy ion bombardment during the growth of epitaxial TiN(100) films by reactive magnetron sputtering: Defect formation and annihilation. Journal of Vacuum Science and Technology A: Vacuum, Surfaces and Films, 1987, 5, 2162-2164.	0.9	4
173	Identification of semi-coherent Y2O3 inclusions in YBa2Cu3Ox superconducting thin films by HREM. Micron and Microscopica Acta, 1992, 23, 231-232.	0.2	4
174	Title is missing!. Journal of Materials Science: Materials in Electronics, 1999, 10, 203-208.	1.1	4
175	Microwave properties of tunable capacitors basee on magnetron sputtered ferroelectric Na0.5K0.5NbO3 film on low and high resistivity silicon substrates. Integrated Ferroelectrics, 2001, 39, 359-366.	0.3	4
176	Nucleation of titanium nanoparticles in an oxygen-starved environment. II: theory. Journal Physics D: Applied Physics, 2018, 51, 455202.	1.3	4
177	Plasma-based processes for planar and 3D surface patterning of functional nanoparticles. Journal of Nanoparticle Research, 2019, 21, 1.	0.8	4
178	Pressure dependence of the resputtering of Y-Ba-Cu-O thin films grown by DC magnetron sputtering. Superconductor Science and Technology, 1991, 4, S379-S381.	1.8	3
179	Transmission electron microscopy of epitaxial SrTiO3 films on LaAlO3 substrates. Microelectronic Engineering, 1995, 29, 309-312.	1.1	3
180	Hydrogen sensing by NKN thin film with high dielectric constant and ferroelectric property. Sensors and Actuators B: Chemical, 2005, 108, 490-495.	4.0	3

#	Article	IF	CITATIONS
181	Nucleation of titanium nanoparticles in an oxygen-starved environment. I: experiments. Journal Physics D: Applied Physics, 2018, 51, 455201.	1.3	3
182	Growth, structure and properties of TiN coatings on steel substrates. AIP Conference Proceedings, 1986, , .	0.3	2
183	The influence of target oxygen on the YBa2Cu3O6+l̂′ directâ€current magnetron sputtering process. Journal of Vacuum Science and Technology A: Vacuum, Surfaces and Films, 1991, 9, 2165-2169.	0.9	2
184	Spontaneous conductance fluctuations and percolation in YBa/sub 2/Cu/sub 3/O/sub 7/ thin films. IEEE Transactions on Magnetics, 1993, 29, 3574-3576.	1.2	2
185	Study of magnetoresistance in oriented YBa2Cu3O7â <sup>~°</sup> Î <sup>~</sup> thin film. Physica B: Condensed Matter, 1994, 194-196, 2291-2292.	1.3	2
186	Microstructure of SrTiO <sub>3</sub> Thin Films as Single Layer and Incorporated in Yba <sub>2</sub> Cu <sub>3</sub> O <sub>7-x</sub> /SrTiO <sub>3</sub> Multilayers. Materials Research Society Symposia Proceedings, 1995, 401, 369.	0.1	2
187	Ionized-PVD by pulsed sputtering of Ta for metallization of high-aspect-ratio structures in VLSI. , 0, , .		2
188	RF-Magnetron Sputtered Au/(Na,K)NbO3/SiO2/Si MFIS-diode Structures. Materials Research Society Symposia Proceedings, 2001, 688, 1.	0.1	2
189	Semi-Coherent Yttria Inclusions Occurring Spontaneously in YBa <sub>2</sub> Cu <sub>3</sub> O <sub>6+×</sub> Films Grown by Dc Magnetron Sputtering. Materials Research Society Symposia Proceedings, 1992, 275, 389.	0.1	1
190	Conductance noise in YBCO thin films. Physica B: Condensed Matter, 1994, 194-196, 1635-1636.	1.3	1
191	Low temperature growth of SrTiO3thin films on glass fiber laminate substrates. Ferroelectrics, 1999, 225, 287-294.	0.3	1
192	Quantum design and synthesis of a boron–oxygen–yttrium phase. Applied Physics Letters, 2003, 82, 4286-4288.	1.5	1
193	Effect of chemical composition on the elastic and electrical properties of the boron-oxygen-yttrium system studied byab initioand experimental means. Physical Review B, 2004, 69, .	1.1	1
194	Erratum to "Spatial Electron Density Distribution in a High-Power Pulsed Magnetron Discharge― IEEE Transactions on Plasma Science, 2005, 33, 1129-1129.	0.6	1
195	Characterisation of Nanoparticle Structure by High Resolution Electron Microscopy. Journal of Physics: Conference Series, 2014, 522, 012065.	0.3	1
196	Iron Oxide Nanoparticle Decorated Graphene for Ultra-Sensitive Detection of Volatile Organic Compounds. Proceedings (mdpi), 2018, 2, .	0.2	1
197	Cross-section preparation for tem of film-substrate combinations with large differences in sputtering yields. Ultramicroscopy, 1985, 17, 172.	0.8	0
198	The dc magnetron sputter deposition process of YBa 2 Cu 3 O x thin films. Physica C: Superconductivity and Its Applications, 1989, 162-164, 599-600.	0.6	0

#	Article	IF	CITATIONS
199	Fluctuation magnetoconductivity in an YBa2Cu3O7â~δ thin film. Physica C: Superconductivity and Its Applications, 1994, 235-240, 1925-1926.	0.6	0
200	Characterization of Sputtered Cerium Dioxide Thin Films. Materials Research Society Symposia Proceedings, 1994, 355, 209.	0.1	0
201	Monte Carlo simulations of the transport of sputtered particles. , 0, , .		0
202	Electrostatic powder impact deposition (EPID) of Ge on Si and Cu substrates, microstructure and morphology study. Journal Physics D: Applied Physics, 2000, 33, 1155-1160.	1.3	0
203	Growth and characterization of RuO/sub 2/ films prepared by reactive unbalanced magnetron sputtering. , 0, , .		0
204	Investigation of 4H-SiC diode with RuO/sub 2/ Schottky contact by DLTS. , 0, , .		0
205	The spatial and temporal variation of the electron energy distribution function (EEDF) in the HiPIMS discharge. , 2009, , .		0
206	Publisher's Note: Molecular dynamics simulation of the growth of Cu nanoclusters from Cu ions in a plasma [Phys. Rev. B <b>90</b> , 165421 (2014)]. Physical Review B, 2015, 91, .	1.1	0
207	Complex 3D nanocoral like structures formed by copper nanoparticle aggregation on nanostructured zinc oxide rods. Materials Letters, 2016, 184, 127-130.	1.3	0
208	Phase separation within NiSiN coatings during reactive HiPIMS discharges: A new pathway to grow NixSi nanocrystals composites at low temperature. Applied Surface Science, 2018, 454, 148-156.	3.1	0
209	Reproducible Fabrication of YBa2Cu3O6+ $\hat{l}$ Thin Films by DC Magnetron Sputtering. , 1990, , 93-100.		0
210	Microstructure and microwave loss studies on epitaxial YBa2Cu3Ox thin films. , 1992, , 219-224.		0